Int. J. Environ. Res., 7(1):113-130, Winter 2013
ISSN: 1735-6865

Recovering Plastics via the Hydraulic Separator Multidune: flow analysis and Efficiency Tests

Moroni, M.[1*], La Marca F.[2], Cherubini L.[2] and Cenedese A.[1]

[1]Department of Civil and Environmental Engineering, Sapienza University of Rome, via Eudossiana, 18 – 00184, Rome, Italy

[2]Department of Chemical Engineering Materials & Environment, Sapienza University of Rome, via Eudossiana, 18 – 00184, Rome, Italy

Received 19 May 2012; Revised 17 July 2012; Accepted 7 Aug. 2012

ABSTRACT: Plastic recycling is the process of recovering scrap or waste plastics and reprocessing the material into useful products that sometimes differ completely in form from their original state. An important issue in plastic recovery and recycling is that plastic waste usually contains a variety of plastics that differ in their physical and chemical properties. Separation of recovered plastics into distinct classes is a fundamental prerequisite for their use as secondary raw materials. The Multidune separator is a hydraulic channel that permits solid particle sorting on the basis of differential transport mechanisms. Steady flow conditions are established within the apparatus. An image analysis technique was employed to reconstruct the trajectories of tracer particles within the fluid and to determine the evolution of the velocity field with time. Pollen and plastic particles were used as tracers. Unlike plastic particles, pollen is expected to passively follow the fluid flow field. Tests on monomaterial and composite samples were conducted while varying the operative conditions, and comparisons were made. The presence of three different recirculation areas occurred regardless of the hydraulic head at the Multidune inlet except for the first and last chambers. The lower recirculation zone is larger than the upper recirculation zone because of geometrical constraints. With variation in the hydraulic head, the geometry of the inner structures does not change appreciably. If a plastic particle within the principal transport path interacts with the lower recirculation area and its physical characteristics (density and dimensions) are such that it remains trapped, the separation process is successful. Because of its smaller dimensions and the reduced value of its velocity field, the upper recirculation area is relatively ineffective in the separation process.

Key words: Plastic recovery, laboratory experiments, image analysis techniques, hydraulic separation, fluid dynamics

INTRODUCTION

Plastic recycling is essential to reduce the accumulation of material in landfills and to decrease the production of raw materials. In fact, in industrialized countries, plastics represent one of the largest categories of municipal solid waste (Shent *et al.*, 1999). The global consumption of plastics was reported to be 230 million tons in 2009 (PlasticsEurope, 2010), of which 55 million tons were produced in Europe. Of the current European demand for plastics, 75% is represented by five high-volume types of plastics; these are polyethylene, including low density (PE-LD), linear low density (PE-LLD) and high density (PE-HD), polypropylene (PP), polyvinyl chloride (PVC), polystyrene (solid PS and expandable PS) and polyethylene terephthalate (PET). The most commonly used types of resins are polyolefins (PE-LD, PE-HD, PE-LLD and PP); together, these four resins account for approximately 50% of plastic demand. PVC is the third largest resin type at 11%. Of the plastics produced in Europe, 24.3 million tons were reported as having been collected as waste. Of this collected waste, 5.5 million tons were recycled as manufacturing feedstock (22.5%) and 7.6 million tons went into energy recovery (31.5%), with the balance (11.2 million tons) probably being disposed of primarily in landfills (PlasticsEurope, 2010). Global consumption is increasing (PlasticsEurope 2007a) while material amount disposed in landfills is slightly lower (PlasticsEurope 2007b).

Plastic materials are currently recycled using two different methods: chemical recycling and mechanical recycling. Chemical recycling is driven by thermal (e.g.,

*Corresponding author E-mail: monica.moroni@uniroma1.it

pyrolysis) or chemical (selective solvents) processes that essentially break down the original polymer chains and molecules within the original material (Jody and Daniels, 2010). Conversely, mechanical recycling generally consists of shredding old products into small pieces followed by the use of separation units to extract specific sizes or materials from the main material flow (e.g., magnetic drums to separate ferrous metals and sophisticated sorting techniques such as infra-red scanning); mills and extruders are then used to convert the separated plastics into new machine-ready granules. Mechanical recycling is now the primary method used to recycle thermoplastic polymers. However, mechanical recycling of thermosetting polymers is not feasible because heat can result in their carbonization.

The success of the mechanical recycling of thermoplastic polymers and the quality of the products that can be manufactured from the recycled material largely depend on the efficiency of the manual or automatic separation stage (Gent *et al.*, 2009). Depending on the type of plastic waste involved, secondary raw materials of various kinds that are suitable for a variety of uses can be obtained. To this end, mechanical recycling can be carried out as either heterogeneous or homogeneous recycling based on the desired quality of the secondary raw material to be obtained. In heterogeneous recycling, the goal is to obtain a low-quality mixed material composed of PE, PP, PS, PET and traces of PVC. In this case, the separation phase is aimed only at eliminating non-plastic materials that may be present in the waste stream. Homogeneous recycling, on the other hand, is the processing of a single type of thermoplastic polymer so that it is obtained free of contamination from other polymers, inert fillers or additives that may affect the quality and workability of the end product. In homogeneous recycling, the efficacy of the separation process plays a major role. The main problem in homogeneous recycling is related to the narrow range of variation of the specific mass of plastic materials (0.9-1.5 g/cm^3) (Plastics International, 2007). Particularly relevant is separating PVC from PET. PVC is considered an extremely dangerous contaminant because, if warmed to high temperatures in unsuitable facilities, it frees chlorine-based carcinogenic compounds such as dioxins and furans. Although the separation of PVC from PET (the latter is more abundant in urban wastes than the former being the most favourable packaging material world-wide for beverages (Welle, 2011)) is often conducted using automatic sorting (Dinger, 1992; Ahmad, 2004), gravity separation, electrostatic separation and froth flotation (Buchan and Yarar, 1995; Hearn and Ballard, 2005; Wei and Realff, 2005; Kinoshita *et al.*, 2006; Menèndez *et al.*, 2007; Tilmatine *et al.*, 2009; Sadat-Shojai and Bakhshandeh, 2010) all have limitations in terms of operating costs and production capacity. The Multidune separator, hereinafter referred to as 'Multidune', allows one to overcome the above-mentioned inconveniences. Multidune consists of a hydraulic channel that allows solid particles to be sorted on the basis of differential transport mechanisms. The name Multidune was chosen due to the undulating profile of the channel, which reproduces the typical shape of desert dunes (De Sena *et al.*, 2008 hereinafter DS2008). The Multidune, which has been developed at the laboratory scale, fits into the context of plastics recycling as an inexpensive alternative to traditional methods due to its capability of effectively separating plastic particles having a density slightly higher than water.

Controlled laboratory experiments have been conducted in the past to characterize the fluid dynamics field within the Multidune apparatus employing Particle Tracking Velocimetry (PTV) (DS2008). The main results presented in DS2008 consist in the description of the two velocity components and of the three characteristic regions developing within chamber C3 of the Multidune. The experimental technique employed here (Feature Tracking - FT) represents an important step forward respect to PTV for the possibility to analyze images with high density of tracer particles and to compute robust statistics. For details and comparisons between the two image analysis techniques refer to Moroni and Cenedese (2005). Through the use of a more powerful experimental equipment, the velocity field in the entire apparatus was reconstructed allowing the full characterization of the fluid behavior within the eight chambers to be achieved. To facilitate the comparison of the velocity fields, color maps and vertical profiles are presented for the eight chambers and five hydraulic heads. It was next verified if the three characteristic regions develop in all chambers and if differences arise. The accurate reconstruction of the fluid dynamics of water flowing through the apparatus allows the behavior of plastic particles to be rationally correlated to the velocity field features. As far as it concerns the separation tests, most of the plastic particles employed in DS2008 have been used for the separation tests presented here. Plastic specific mass has been recomputed with a more accurate procedure than before.

This work consists of three parts. In the first part, we investigated the fluid dynamic behavior of the Multidune apparatus using high spatial and temporal resolution image analysis systems and passive tracer particles, i.e., particles of sizes on the order of one hundred microns with a density equal to that of water

(Section 3.1). In the second part, we investigated the behavior of two types of plastic particles (PS and PVC, hereinafter referred to as active tracers); the same particles were used afterwards in separation tests under the same experimental conditions (Section 3.2). The third part describes tests on composite plastics (Section 4).

MATERIALS & METHODS

The Multidune apparatus is constructed from a sequence of eight parallel cylindrical tubes (30 mm diameter) welded together in a plane (Fig. 1). The complex is sliced along its lateral mid-plane, and the lower half is shifted laterally and then fixed relative to the upper half. The channel transverse cross-section is rectangular. The apparatus is constructed of transparent plastic (Perspex) to guarantee optical access. The shape of the spatially periodic walls (dunes) allows the fluid flowing through the channel, usually water, to experience strong accelerations and to form recirculation zones of low velocity that facilitate the separation of solid material in suspension.

In Fig. 1, the eight chambers within the apparatus are labeled according to their positions along the flow direction [C1 (first chamber), C2…C8 (last chamber)]. Flow is provided in a lateral direction normal to the axis of the cylindrical tubes through inlet holes on one side of the complex and outlets on the opposite side. The first chamber of the channel has eight round input nozzles (I1, I2…I8), and the last chamber has 8 round output nozzles (O1, O2…O8) that are positioned symmetrically with respect to the inlet nozzles. Settled effluxes can be collected in the lower complex from each half-cylinder collection nozzle (R1, R2…R8). The presence of a discharge system in every chamber is required for separately collecting the material settled in each chamber. Each of the outlet and collection nozzles has a special tube with a tap in the downstream direction that can be used to disconnect it from the stream.

The Multidune is filled via a variable height reservoir; the output of the reservoir is split so as to distribute water through the 8 inlet nozzles (Fig. 1). The water level within the tank is controlled through

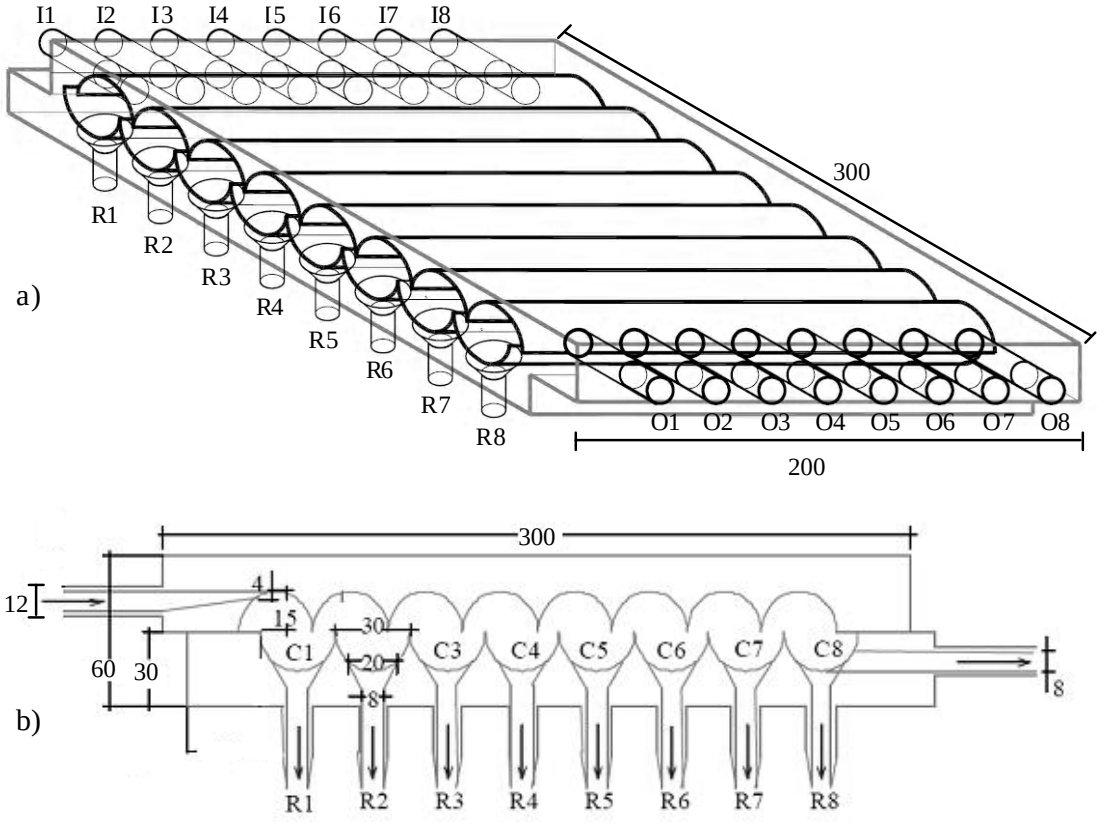

Fig. 1. a. 3-D representation and b) longitudinal section of the Multidune apparatus. C indicates the 8 chambers, R the 8 collection nozzles, I the 8 inlet nozzles and O the 8 outlet nozzles. Lengths are expressed in millimeters

an overflow exit. The plastic samples and the tracer for image analysis are introduced through nozzles I3 and I4. The average flow rate depends on the hydraulic head at the inlet nozzles and the number of open outlet nozzles.

Experiments were conducted at five different elevations of the tank (referred to the inlet nozzles' heights, which were 0.84 m, 1.34 m, 1.84 m, 2.34 m, and 2.69 m) and three open outlet nozzles (O2, O4 and O6). Table 1 shows the difference in fluid elevation between the tank and the inlet nozzle centers and the corresponding flow rates. In the following discussion, we use the symbols Q1, Q2, Q3, Q4 and Q5 to indicate inlet nozzle heights as well as flow rates.

All tests conducted employed a procedure consisting of the following steps:

1. adjustment of the water tank height
2. water supply through all 8 inlet nozzles
3. aperture of the output nozzles (O2, O4 and O6)
4. passive tracer or sample injection into the apparatus
5. test execution (during separation tests, the material expelled from the output nozzles is recovered)
6. closure of the output nozzles
7. recovery of material from each chamber
8. drying of recovered materials prior to weighing.

The operational conditions ensure the achievement of an almost two-dimensional flow field along the longitudinal cross-section passing through the center of the apparatus.

Table 1. Difference in fluid elevation between the tank and the center of the Multidune inlet nozzles and corresponding flow rates

	Difference in fluid elevation between tank and Multidune (m)	Average flowrate (L/min)
Q_1	0.84	9.35
Q_2	1.34	10.69
Q_3	1.84	11.82
Q_4	2.34	12.98
Q_5	2.69	13.53

The image acquisition system consists of the following three components:

- a high-speed, high-resolution camera (Mikrotron EoSens) equipped with a Nikon 50- mm focal length lens; the camera captures gray-scale images at up to 500 fps with a resolution of 1280×1024 pixels. For the present set of measurements, images were acquired at 250 fps.
- a high-speed Camera Link DVR operating in Full configuration (IO Industries DVR Express® Blade) to manage data acquired by the camera;
- a large-capacity disk array (4 Tbyte) to store images. Due to the consistent video data throughput (up to 600 Mbyte/s), the disk array is connected to the DVR through optical fibers.

Proper illumination is ensured through the use of a 150 W Intralux lamp connected to a 40-cm-long linear optical fiber positioned at the Multidune top. A light sheet oriented in the longitudinal direction, i.e., parallel to the mean flow field is generated. One camera and a planar light sheet are mandatory for the application of a two-dimensional image analysis technique.

Different types of particles, all of which are characterized by a remarkable capacity of reflecting light, have been used as tracers. The tracer particles included the following:

- pine pollen particles with a diameter of about 80 μm; these assume the same specific weight of the liquid and perfectly follow the fluid motion (passive tracer);
- PVC particles with a diameter of about 250 μm and specific weight of 1.350 g/cm^3; due to the small size of these particles, they follow the fluid motion with a good approximation (passive tracer);
- PS plastic particles of diameter ranging from 0.85 mm to 1.00 mm and density 1.043 g/cm^3; these were also employed in the separation experiments (active tracer);
- PVC plastic particles of diameter ranging from 0.85 mm to 1.00 mm and density 1.353 g/cm^3; these were also employed in the separation experiments (active tracer).

Images were acquired in three different situations:

- camera acquisition window coincident with the entire longitudinal section of the Multidune apparatus, pollen particles used as the tracer and five different heights of the water supply tank, i.e., five different flow rates (Fig. 2a, Series #1);
- camera acquisition window limited to chambers C3, C4, C5 and C6; PVC particles used as the tracer and five different heights of the water supply tank set (Fig. 2b, Series #2);
- camera acquisition window coincident with the entire longitudinal section, PS and PVC plastics used as the tracer and two water supply tank heights, Q1 and Q5 (Fig. 2c, Series #3).

The duration of each experiment was approximately 60 s, i.e., the time required for the particles introduced through the inlet nozzles to pass through the test section.

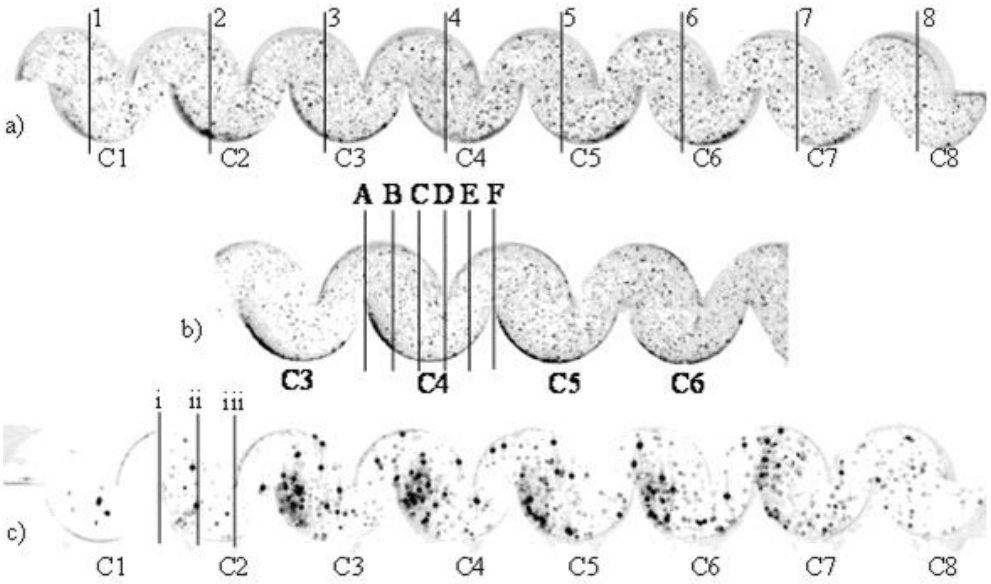

Fig. 2. Negative of one image each from (a) Series #1, (b) Series #2 and (c) Series #3 acquired with the high-speed camera. The figure presents eight profiles (1-8) distributed along the longitudinal section, six profiles (A-F) distributed within C4 and three profiles (i-iii) within C2, along which the two velocity components have been computed

The aim of the investigation was to reconstruct the trajectories of tracer particles seeding the fluid under investigation and to determine the velocity field evolution with time by means of image analysis techniques. Optical methods (i.e., Laser Doppler Anemometry, Particle Image Velocimetry, Particle Tracking Velocimetry, and Feature Tracking) are ideal or quasi-ideal absolute measurement systems (i.e., these methods require no calibration). Because no perturbation of the flow field occurs, they represent accurate, non-invasive instruments suitable for simultaneously obtaining the velocity field time history in the whole domain with a resolution smaller than the phenomenon characteristic time and length scales. The main limitations associated with these techniques are the need to design an experimental apparatus equipped with transparent walls to guarantee the optical access and to seed the working fluid, which must be transparent as well, with tracer particles.

The different particle imaging-based techniques that permit multi-point velocity measurements use images of different densities. Low-density images are generally approached from a Lagrangian point of view with Particle Tracking (PT) techniques (La Porta *et al*., 2001; Moroni *et al*., 2003; Shindler *et al*., 2010, among others). Medium-high density images are usually analyzed by means of Particle Image Velocimetry (PIV), which reconstructs the Eulerian velocity field on a regular, equi-spaced grid (Niblack, 1986; Adrian, 1991; Nogueira *et al*., 2001; Raffel *et al*., 2007, among others). In this study, we employed Feature Tracking (FT), a Particle Tracking (PT) algorithm that permits the user to ignore the constraint of low seeding density. This algorithm can provide accurate displacement vectors even when the number of tracer particles within each image is very large (Moroni and Cenedese, 2005). FT reconstructs the displacement field by selecting image features (image portions that are suitable for tracking because they remain almost unchanged over small time intervals) and tracking these from frame to frame. The matching measure used to follow a feature (and the L×H window around the feature, where L and H are the horizontal and vertical dimensions, respectively) and its "most similar" region at the successive times is represented by the "Sum of Squared Differences" (SSD) of the intensity values. The displacement is defined as the one that minimizes the SSD (Horn and Schunk, 1981). In Feature Tracking, the algorithm is applied only to points for which the solution for the displacement exists; those points are called "good features to track". FT allows a Lagrangian description of the velocity field that provides sparse velocity vectors with application points coincident with large luminosity intensity gradients, which are likely located along tracer particle boundaries (Moroni *et al*., 2008). Lagrangian data are then used to reconstruct instantaneous and time-averaged Eulerian velocity fields through a resampling procedure. The mean

velocity components along axes x and z, u and w, and their variances, $\overline{u'^2}$ and $\overline{w'^2}$, are evaluated in the knots of a regular grid of 34 rows and 256 columns. Assuming the phenomenon is stationary as well as ergodic, the ensemble averages are evaluated as temporal averages over a time interval equal to the entire recording time of about 15000 frames. The velocity variances along the axes x and z can be represented by a single image that contains information on both the axes; this image represents the two-dimensional turbulent kinetic energy.

$$TKE2D = \left(\overline{u'^2} + \overline{w'^2}\right)/2$$

RESULTS & DISCUSSION

Figs 3a and 3b show the trajectories reconstructed by the FT algorithm for experiments at the lower (Q1) and higher (Q5) flow rates (Series #2). The trajectories, which correspond to a visualized overlapping of the 32 consecutive positions of the tracer particles, extend over a time interval of about 0.13 s. A direct picture-to-picture comparison can be made. The colors range from blue, which is associated with the first time shown, to red, which is associated with the last time shown. The principal current and two recirculation areas are evident in both pictures. Comparison of the two images demonstrates the increased length of the trajectories reconstructed at the higher flow rate. The increased length of the trajectory segments increases the density of information displayed in Fig. 3b.

Figs 5-6 present the velocity field for the entire apparatus (images of Series #1) and for chamber C4 (images of Series #2) as a function of the hydraulic head at the Multidune inlet.

In particular, Figs 4a and 4b report velocity vectors that have been overlapped with the color map of the horizontal velocity component for flow rates Q_1 and Q_5, respectively. For a better understanding of the flow field, Figs 5a and 5c shows two enlarged views of the previous figures framing chamber C4. Figs 4c and 4d present the velocity vectors overlapped with the color map of the vertical velocity component. The

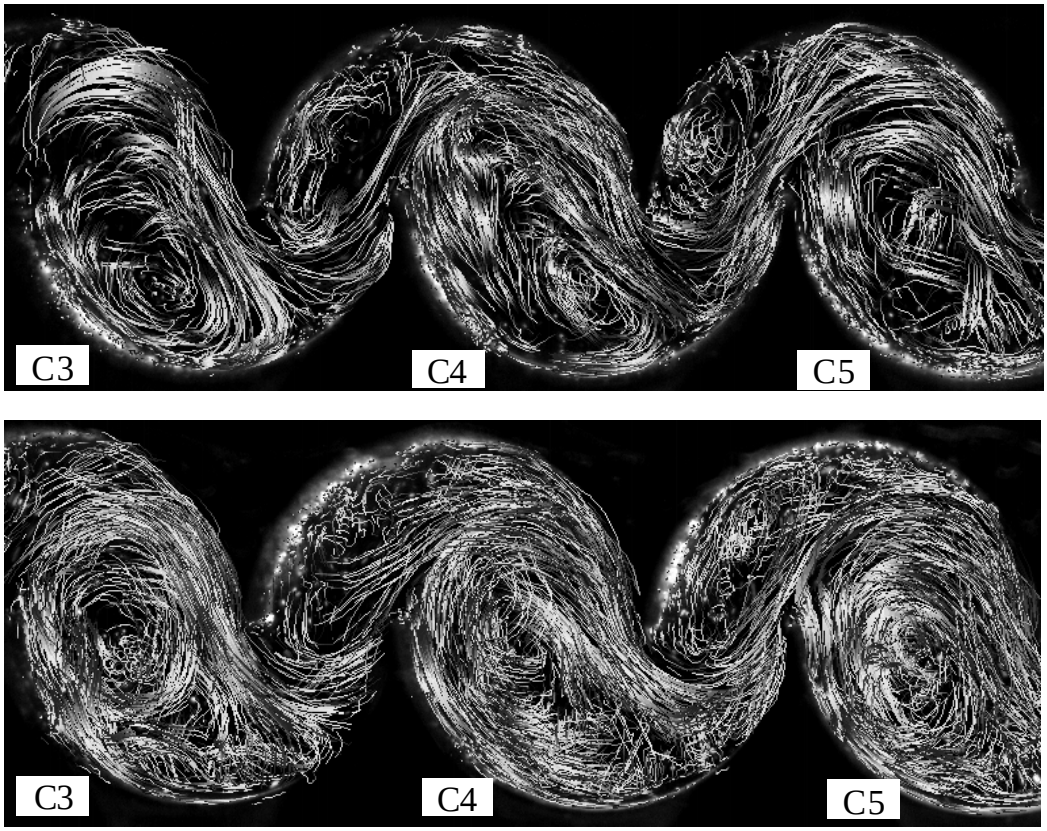

Fig. 3. Trajectories reconstructed by the Feature Tracking algorithm for experiments at the (a) lower (Q_1) and (b) higher (Q_5) flow rates. In both figures, chambers C3, C4 and C5 are indicated. The colors range from dark grey, which is associated with the first time shown, to light gray, which is associated with the last time shown

corresponding enlarged views are shown in Figs 5b and 5d. Figs 5e and 5f shows the turbulent kinetic energy for chamber C4 at the same flow rates.

The velocity fields in C4 (Fig. 5) present a better definition due to the higher spatial resolution of the acquired images (these images were obtained at the same camera resolution using a smaller acquisition window). The streamlines for the lower and higher flow rates show the characteristic behavior of the fluid flowing through the separator (Fig. 6).

The analysis of the velocity fields and the streamlines suggests that the fluid dynamic behavior of the Multidune apparatus is characterized by the following three predominant areas:

-the principal transport flow, where the fluid is characterized by a positive value of the velocity component along the x axis in the entire longitudinal section. The principal transport flow is responsible for the transport of particles from one chamber to the next; it eventually drives material to the outlet nozzles without separation. It is indicated by red streamlines in Fig. 6.

-the lower recirculation zone, visible below the principal current in each of the height chambers. Its clockwise rotating motion is suitable for capturing particles from the principal current. It is expected that plastic particles captured in this way will behave in one of the following ways:

- settle within the chamber if sufficiently heavy;
- follow the upward portion of the rotating motion without again reaching the principal current, due to the fact that they are too heavy to perform a complete rotation;
- execute a complete rotation and be recaptured by the principal transport flow to settle in the next chamber or be expelled.

The particle behavior within the recirculation zone is influenced by its density and dimension as well as by the presence of a vortex. This behavior is indicated with green streamlines in Fig. 6.

-the upper recirculation zone, visible above the principal transport current. The purpose of the upper recirculation zone is to subtract particles from the principal current and to transfer them to the preceding chamber. To undergo such transfer, particles must move across the principal current and settle in the lower recirculation area of the previous chamber. The particle physical attributes and the characteristic velocity of the principal current will influence the efficacy of this process. This process is indicated by blue streamlines in Fig. 6.

Figs 7a and 7b show the horizontal and vertical velocity components along profiles A to F when Q3 is the flow rate within the Multidune apparatus. Profile A describes the velocity field that is established in correspondence with the lower cusp at the entrance to C4. The velocity components are both positive, and the vertical component is slightly larger than the horizontal one. This is due to the upward movement of the main transport current entering chamber C4. It can be seen that the velocity behavior along profile F substantially collapses with that along Profile A. Profile B accounts for the main transport current velocity distribution (upper part of the curve) and for the lower recirculation area (central and lower parts of the curve). In Profile B, the horizontal velocity component changes sign while the vertical component remains positive. The same comments hold for Profile C except for the altered sign of the vertical velocity component due to the downward direction of the principal transport current. Profile D corresponds to the upper cusp within C4. Here, the main transport current direction is downward, and the velocity field magnitude is comparable to that in other sections of C4. Profile E intersects the upper recirculation area, which justifies the change of sign of both velocity components.

Observation of the velocity field within the Multidune apparatus (Fig. 4) suggests that the lower recirculation area is not completely developed in chambers C1 and C8. This is especially true in C1, where the fluid enters the apparatus; in this region, the current is less well organized than in the region ahead. It can be seen that, in terms of dimensions and velocity values, chambers C3, C4, C5 and C6 present analogous recirculation areas at each reference hydraulic head. This is further confirmed by the horizontal velocity component profiles presented in Figs 7c and 7d. At both the lower and higher flow rates, the profiles in C3, C4, C5 and C6 nearly collapse. The profiles that deviate the most are those in C1 and C8.

The fluid vein characterizing the principal current presents an inner part with velocity and kinetic energy increasing with the hydraulic head. Nevertheless, the characteristic dimension of the principal current remains practically constant for all the flow rates employed. At each flow rate, the upper recirculation zone presents values of the velocity field, i.e., the vorticity field, that are significantly lower than the characteristic velocity in the principal current. For this reason, this zone is ineffective in capturing particles from the mail transport path and thus is ineffective in the separation process. It is expected that upon further reducing the flow rate or modifying the inner geometry of the apparatus the upper recirculation zone will play a role in the separation process. The results obtained by modifying the geometry of the apparatus are presented in La Marca et al. (2011).

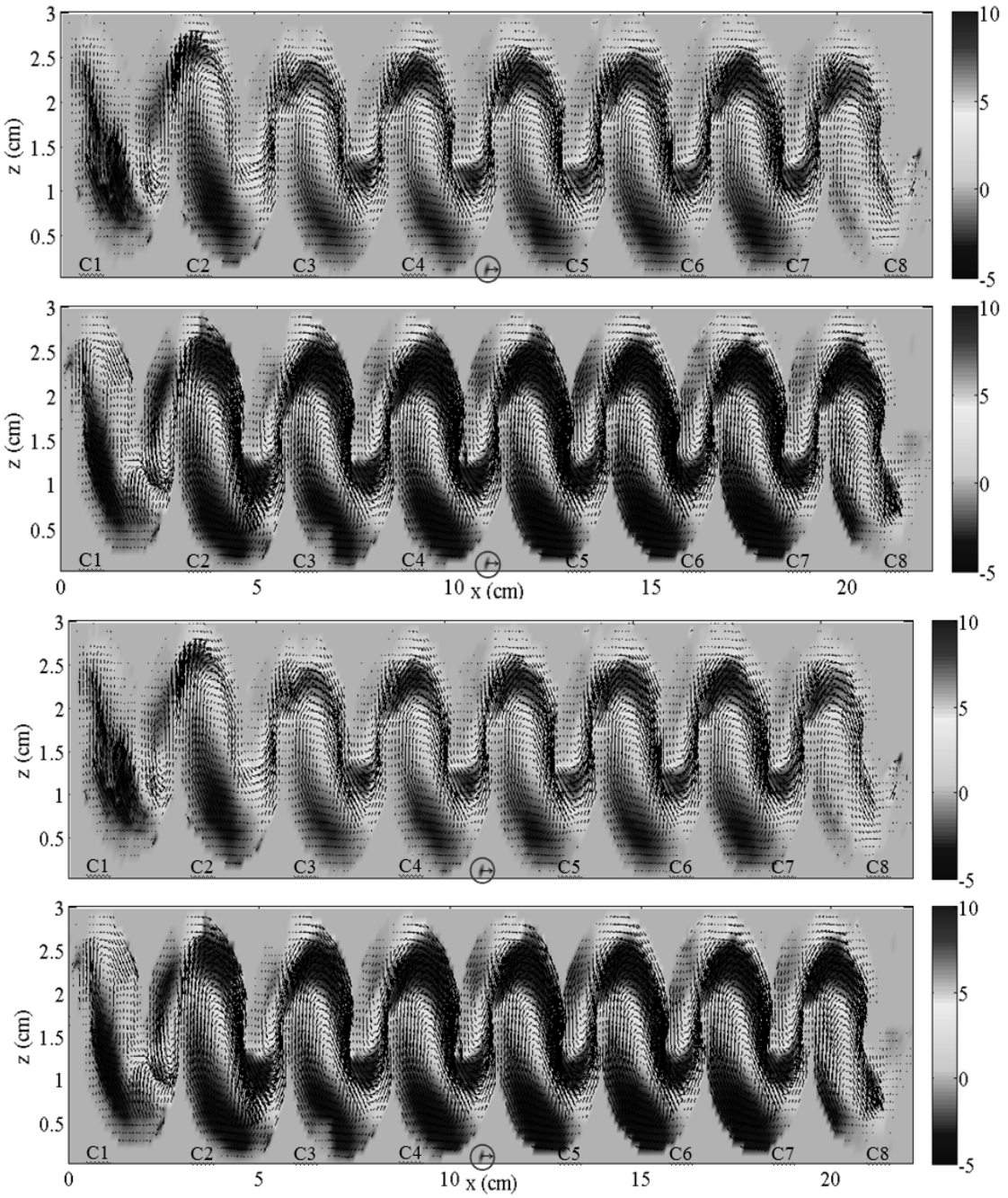

Fig. 4. Eulerian velocity vectors and map of colors of the horizontal velocity component at the (a) lower (Q1) and (b) higher (Q5) flow rates; vertical velocity component at the (c) lower (Q1) and (d) higher (Q5) flow rates. The reference velocity vector (red circle) is equal to 10 cm/s

The velocity field in the lower recirculation area, which is larger than that in the upper recirculation zone, is in each case significantly lower than the characteristic velocity in the principal current. When the flow rate is increased, the velocity within the lower recirculation zone increases, especially in the ascending portion of the vortex. The drag of settled particles toward the principal current is then facilitated, and separation appears less effective.

A comparison of the streamlines obtained from the velocity fields at low and high flow rates further demonstrates the substantial invariance of the shape and dimension of the zones into which the flow field is

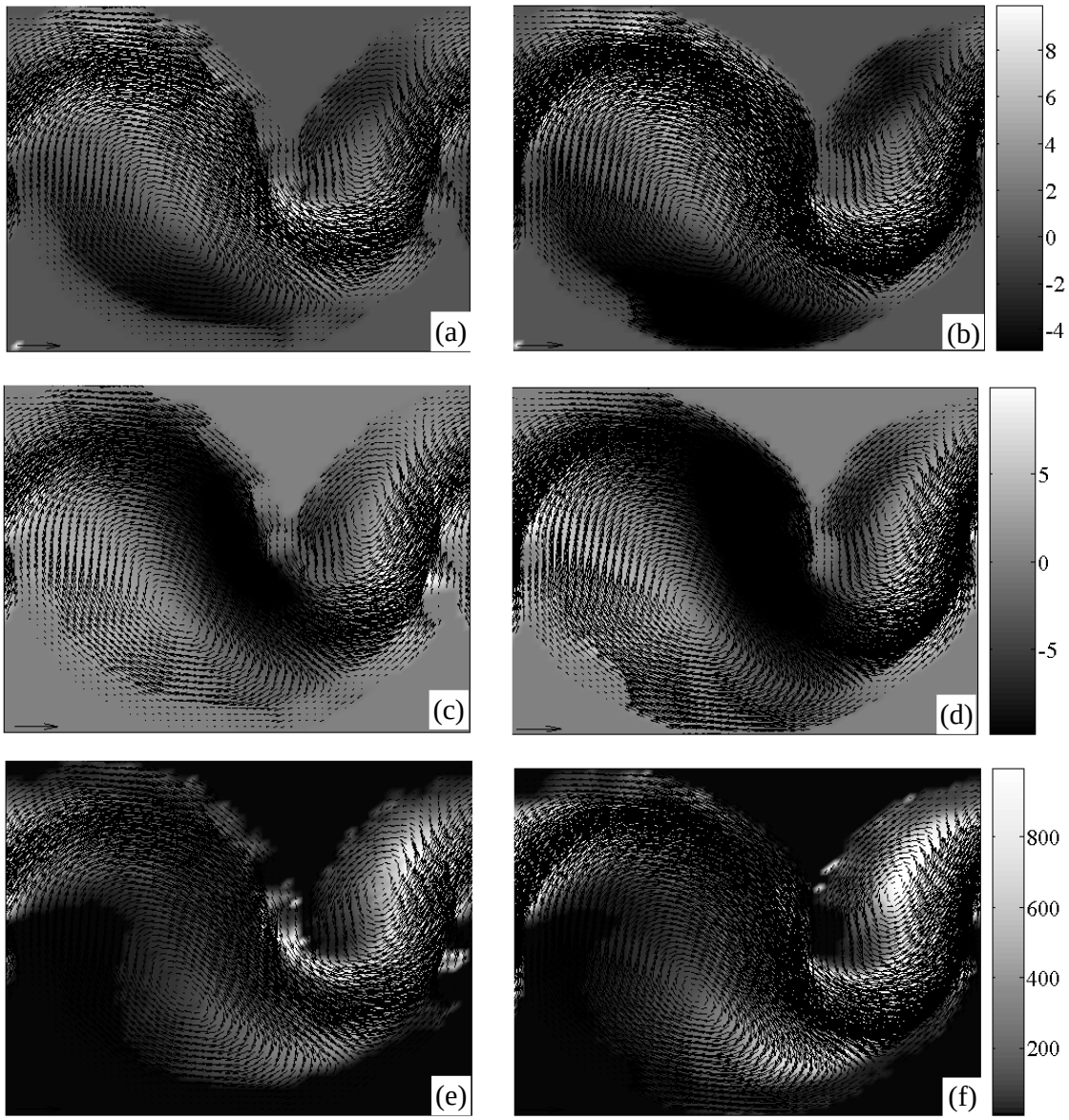

Fig. 5. Eulerian velocity vectors and color map of the horizontal velocity component within chamber C4 at the (a) lower (Q1) and (b) higher (Q5) flow rates; vertical velocity component within chamber C4 at the (c) lower (Q1) and (d) higher (Q5) flow rates; two-dimensional turbulent kinetic energy within chamber C4 at the (e) lower (Q_1) and (f) higher (Q_5) flow rates

organized. On the other hand, the observed streamlines confirm that the region of exchange between the principal current and the upper and lower recirculation zones is enhanced when the flow rate is increased. This increases the probability of interaction between particles that are eventually captured by the upper and lower vortices and the principal flow path and reduces the separation efficacy of the apparatus.

An increase in the flow rate results in a significant increase in the turbulent kinetic energy of the principal current and a much smaller increase in kinetic energy in the recirculation areas. The significantly different behavior of the fluid portion belonging to the principal current at its entrance in a new chamber at the two extreme flow rates should be emphasized. The interaction of the principal current with the lower recirculation area produces a considerably higher level of turbulence at the higher flow rates, disturbing the separation process.

In summary, analysis of the fluid dynamic field that develops within the Multidune apparatus suggests that increasing the hydraulic head augments the

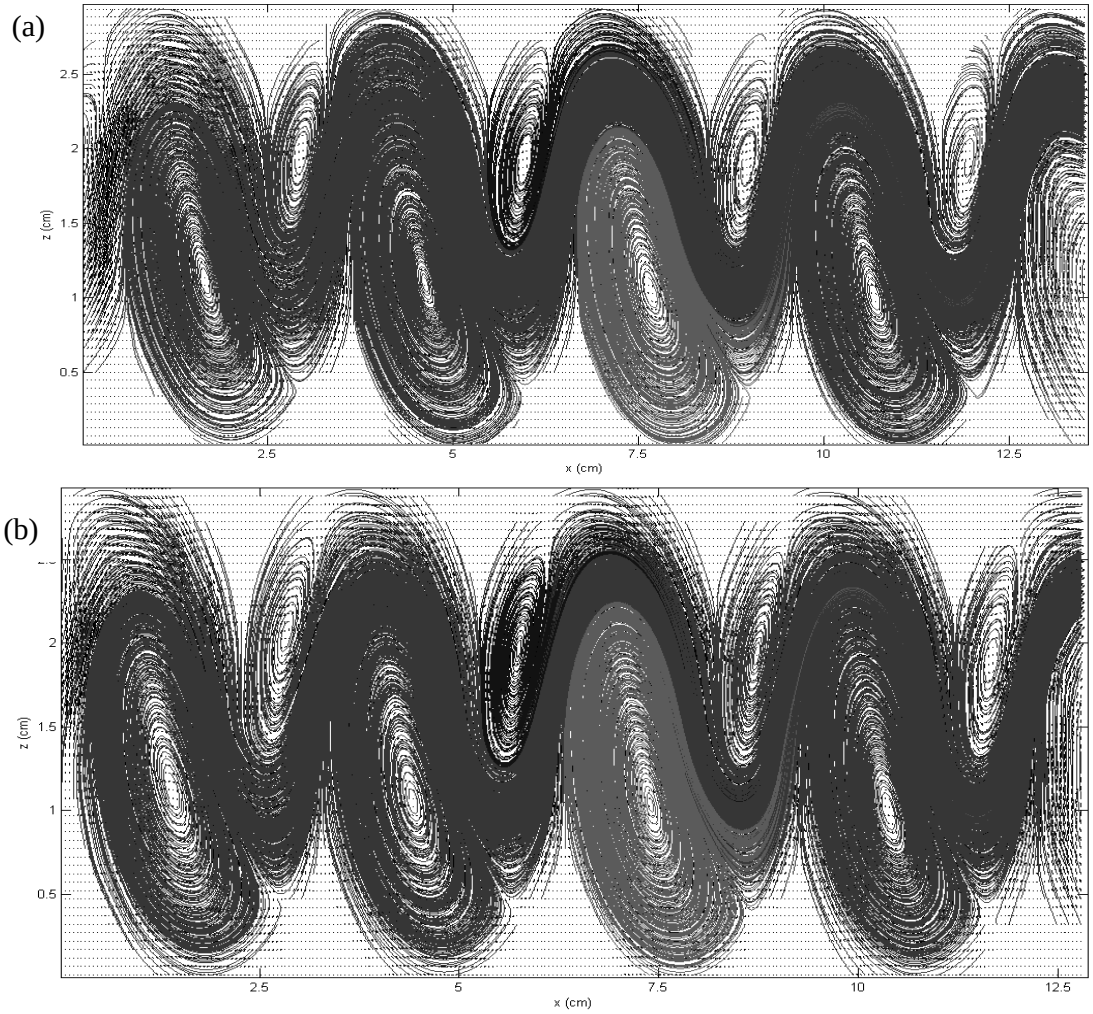

Fig. 6. Streamlines at hydraulic head (a) Q1 and (b) Q5

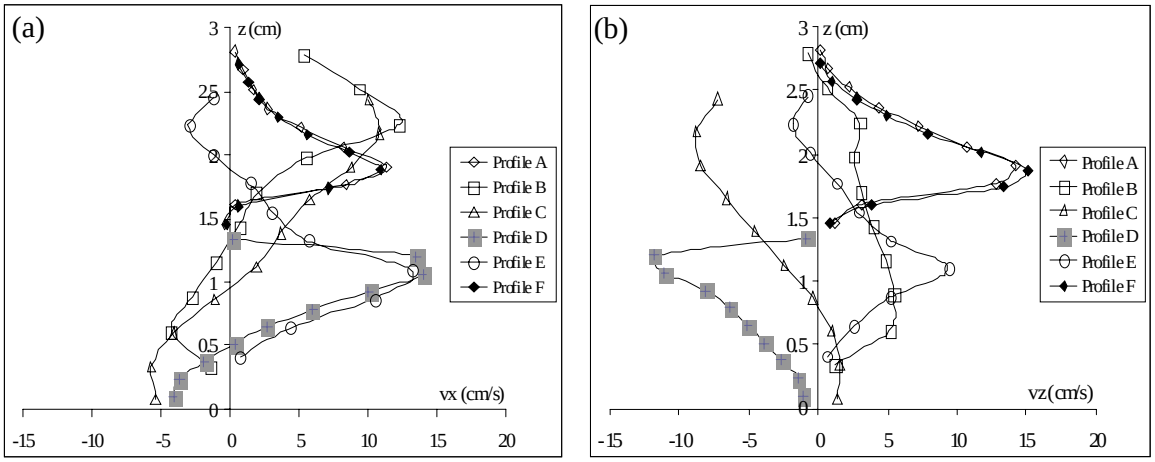

Fig. 7. (a) Horizontal and (b) vertical velocity components along profiles A through F (see Figure 2b) at hydraulic head Q3; horizontal velocity component along profiles 1 through 8 (see Figure 2a) at the hydraulic heads (c) Q1 and (d) Q5; velocity components along the (e) horizontal and (f) vertical directions at hydraulic head Q1 along profiles i through iii (see Fig. 2c) (Contines)

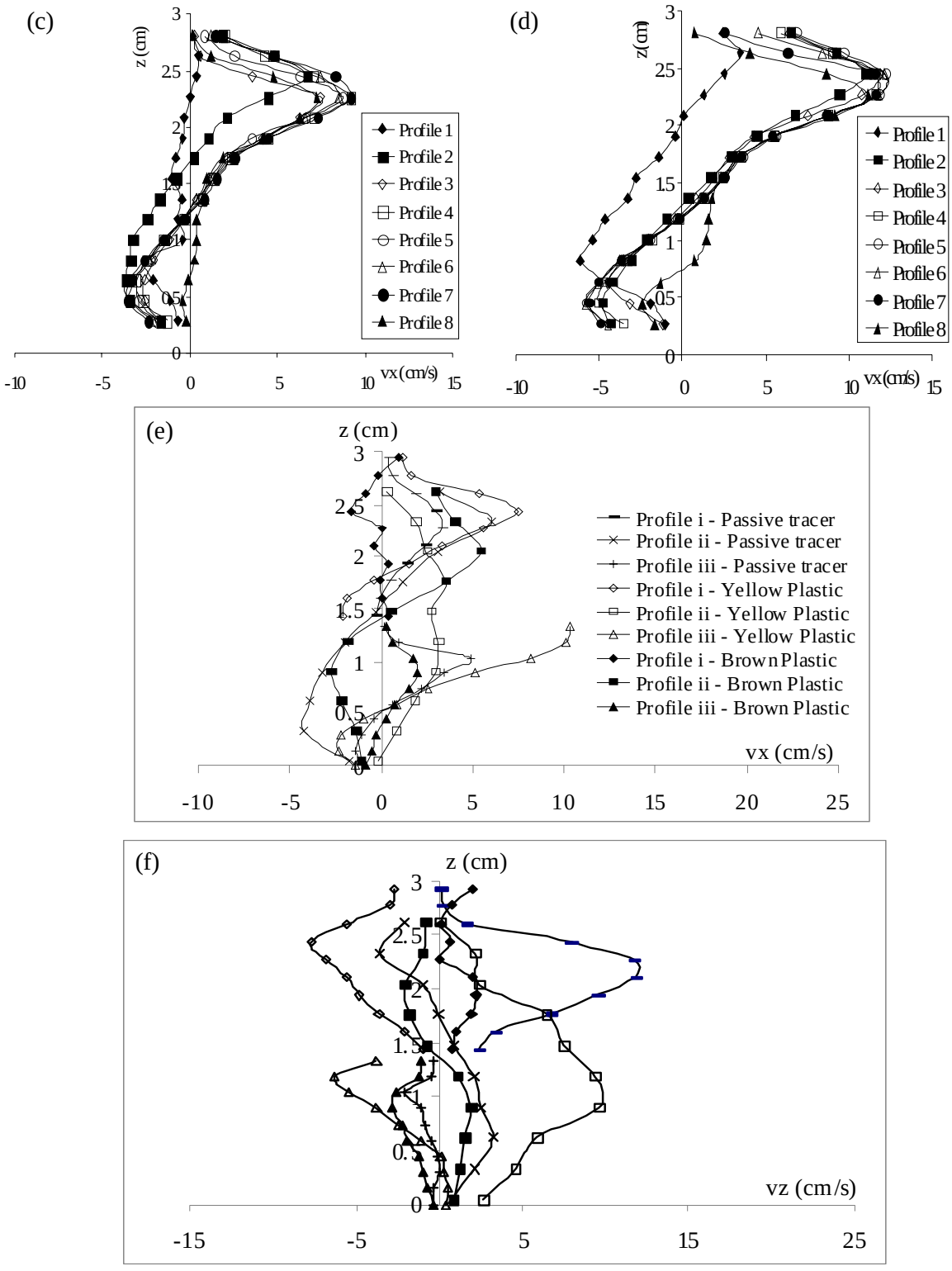

Fig. 7. (a) Horizontal and (b) vertical velocity components along profiles A through F (see Figure 2b) at hydraulic head Q3; horizontal velocity component along profiles 1 through 8 (see Figure 2a) at the hydraulic heads (c) Q1 and (d) Q5; velocity components along the (e) horizontal and (f) vertical directions at hydraulic head Q1 along profiles i through iii (see Fig. 2c)

transport effectiveness of the main current without improving the capture feasibility of the upper and lower recirculation zones. Thus, when the hydraulic head and the transiting flow rate are both increased, the apparatus will lose its effectiveness in separating plastic particles. The eight-chamber design assures plastic particle separation even when C3 is filled with settled material; in that case, the remaining chambers become effective in the separation process.

Feature Tracking was applied to images of Series #3 so that results could be compared with those obtained with the passive tracer. The active tracer consisted of PS and PVC particles of dimensions 0.85-1.00 mm and density 1.043 g/cm^3 and 1.353 g/cm^3, respectively. One reason for the choice of these two resins is the significant difference in their densities. In addition, separation tests using mono-material samples (La Marca et al., 2011) have demonstrated that the behavior of such samples is significantly influenced by the velocity field within the Multidune apparatus. To study the particle behavior in two extreme cases, the acquisitions were carried out using the lower and higher hydraulic heads. To qualitatively visualize the results of those acquisitions, snapshots representing particle trajectories in the initial, intermediate and final stage of each test are shown. Figs 8a-b-c and 8d-e-f show the PS and PVC particle trajectories at the lower flow rate Q1 overlapped with the negative of the acquired image, while Figs 8g-h-i and 8l-m-n show the corresponding trajectories at flow rate Q_5.

Trajectories reconstructed with FT show the extremely different behavior of the two types of plastics. PS particles, which have a density close to that of water, show a behavior much more similar to the behavior of the passive tracer than do the other resins. At hydraulic head Q1, PVC particles settle in

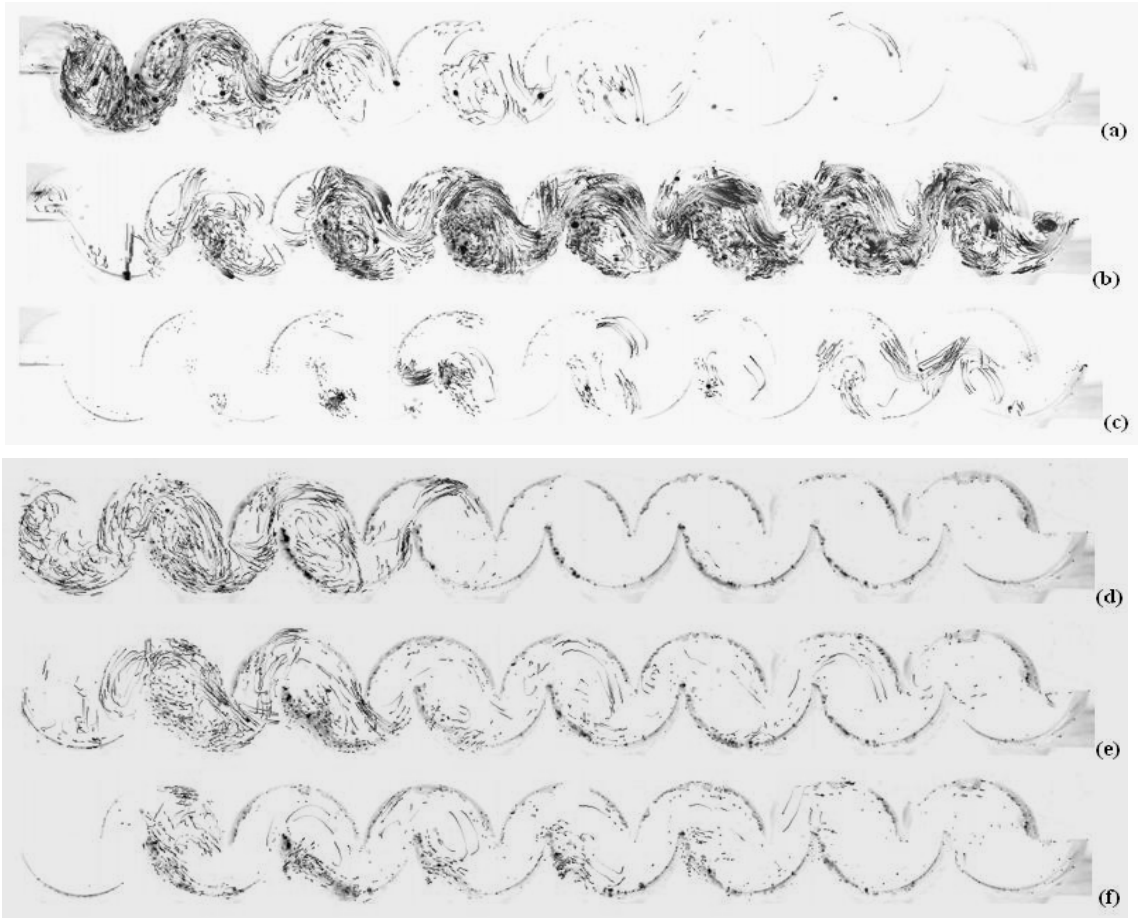

Fig. 8. Snapshots representative of the (a) initial (corresponding to the insertion of the active tracer), (b) intermediate and (c) final stage of the acquisition with PS at hydraulic head Q1; (d) initial, (e) intermediate and (f) final stage of the acquisition with PVC at hydraulic head Q1; (g) initial, (h) intermediate and (i) final stage of the acquisition with PS at hydraulic head Q5; (l) initial, (m) intermediate and (n) final stage of the acquisition with PVC at hydraulic head Q5(Continues)

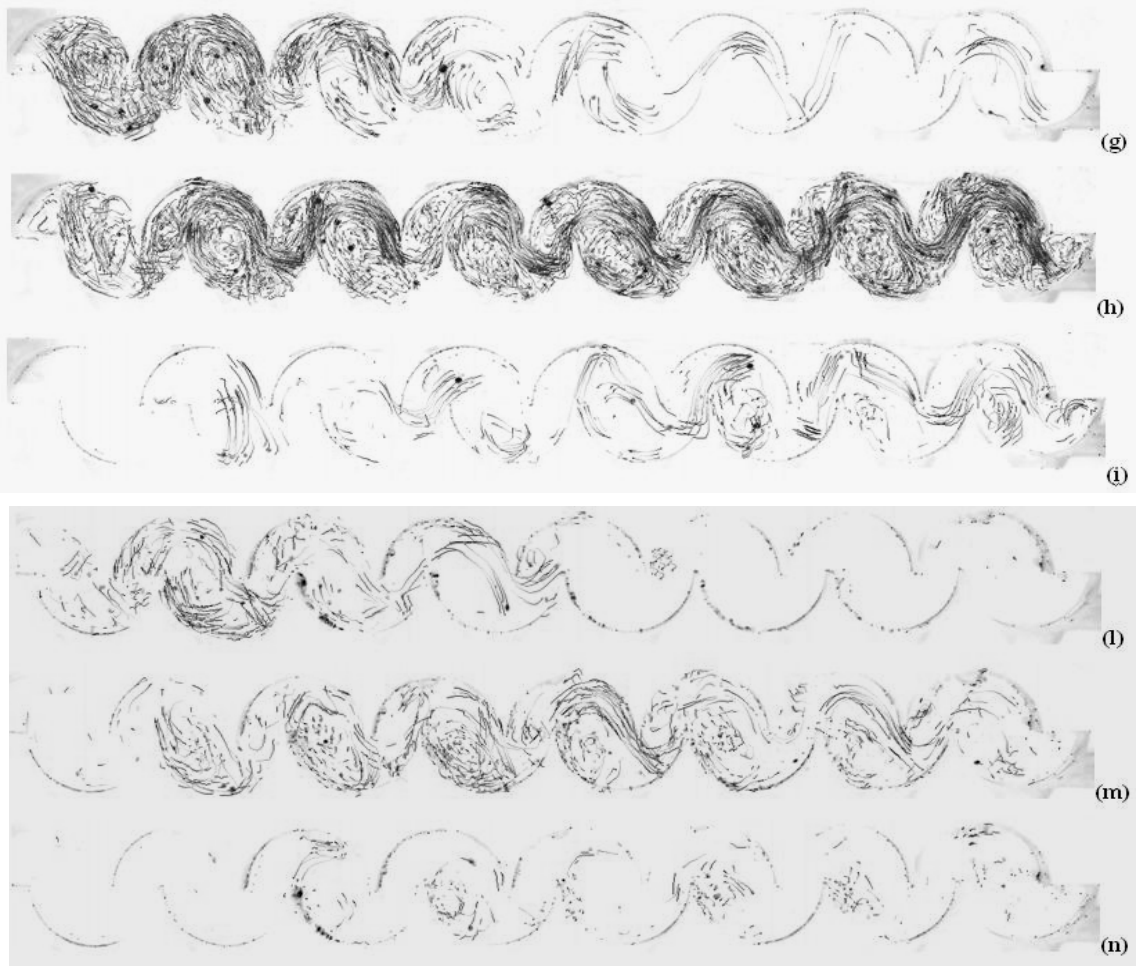

Fig. 8. Snapshots representative of the (a) initial (corresponding to the insertion of the active tracer), (b) intermediate and (c) final stage of the acquisition with PS at hydraulic head Q1; (d) initial, (e) intermediate and (f) final stage of the acquisition with PVC at hydraulic head Q1; (g) initial, (h) intermediate and (i) final stage of the acquisition with PS at hydraulic head Q5; (l) initial, (m) intermediate and (n) final stage of the acquisition with PVC at hydraulic head Q5

the initial chambers. Conversely, PS particles remain in suspension and are finally expelled from the apparatus. When the hydraulic head is increased, even PVC particles tend to follow the principal current and be expelled without settling in any chamber. This is confirmed by separation tests on mono-material samples (La Marca *et al*., 2011).

Observation of the trajectories of the test particles suggests that PS particles, which are totally expelled from the apparatus, do not only follow the path of the principal current but are also regularly captured by the vortical structures. In the region of these structures, light particles are continuously moved upward, where they interact with the principal current. The stronger the updraft, i.e., the higher the hydraulic head, the greater is the probability that the particle will interact with the principal current reaching the next chamber. PVC particles partially follow the rotating motion because, especially at the lower flow rate, the thrust is not strong enough to overcome their weight. Furthermore, the recirculation area is reduced due to material that has settled within and partially filled the chambers. At the higher flow rate, the material does not permanently accumulate within the chamber but instead is gradually renewed until the end of the insertion of material and the final cleaning of the chambers.

Noticeably, PS particles sample the upper recirculation zone more than the passive tracer. This confirms the ineffectiveness of that area in the process of separation.

The horizontal and vertical velocity components along profiles i to iii at the lower flow rate, along with

the behavior of both the passive tracer and the plastic particles, are depicted in Figs 7e and 7f. At both Q1 and Q5, PS particles are totally expelled from the apparatus; in contrast, PVC particles separate only at the lower flow rate. For this reason, we further examined the fluid dynamic behavior of the particles at the lower flow rate. Along profile i, the horizontal velocity component of PVC particles is negative or close to zero, while both the tracer particles and PS plastic particles present a mainly positive profile describing a well-established principal current. A negative velocity is representative of particles unable to proceed downstream, i.e., potentially separating. On the other hand, the vertical velocity component of PVC particles is slightly positive. PVC particles are characterized by a recirculation motion that is more developed than that of the fluid. The behavior of the PS particles is more similar to that of the fluid except for the vertical velocity component along profile i, where the velocity is negative. Along this profile, the particles are already moving toward chamber C2, whereas the fluid still presents an upward motion before the interaction with the upper boundary forces it to enter the next chamber. Along Profile ii, PS plastic particles do not sample the lower recirculation area because both velocity components are positive; this is significantly different from the fluid behavior. Here, PVC plastic particles behave more similarly to the fluid, showing reduced velocity and a different geometry of the recirculation area. In Profile iii, the horizontal and vertical directions for both types of plastic particles and the fluid are more similar, with only slight changes in the magnitude of their velocities.

Tests on mono-material samples (La Marca *et al.*, 2011), while providing useful information on the efficacy of an apparatus, must always be associated with tests on composite samples. Tests of the latter type are needed to understand whether the system is capable of separating different types of plastics in a mixture.

In this study, four samples were used (Table 2). Each sample consisted of two types of plastic particles differing in density and mean diameter. The sizes fell into two ranges, 0.85–1 mm and 1.70–2 mm. All particles presented a quasi-spherical shape, to reduce the influence of such property over the hydraulic behavior. The single plastics were characterized by infrared spectroscopy to determine their typology. The sample consisted of 85% by weight of the useful fraction and 15% by weight of the contaminating fraction. The total weights of the samples were 1.5 g for fine-grained samples (0.85-1 mm) and 2.5 g for coarse-grained samples (1.7-2 mm).

The choice of samples with uneven composition (85% vs. 15%) ensures the realistic nature of the tests. In actual practice, the Multidune would rarely be used for separation of two useful products, but it would often be used to purge one type of plastic (the useful fraction) of a pollutant (contaminating fraction). The sample introduced into the Multidune is separated into two fractions: a fraction in which the useful product is concentrated and a fraction mainly consisting of the contaminating material. If the useful fraction is the heavier one in the mixture, the concentrated product is the material settled in the chambers, while the sterile product is expelled from the separator. Conversely, if the useful fraction represents the lighter of the two

Table 2. Composite sample composition. U identifies the useful fraction, I the contaminating fraction. The total weight for Samples 1 and 2 was 1.5 g, whereas for Samples 3 and 4 it was 2.5 g. PVC: Polyvinyl chloride; PS: Polystyrene; PET: Polyethylene terephthalate

		Plastic typology	Mean density	Particle size distribution	Weight	Percentage of weight
Sample 1						
	U	PVC	1.350 g/cm^3	0.85-1.00 mm	1.275 g	85%
	I	PS	1.043 g/cm^3	0.85-1.00 mm	0.225 g	15%
Sample 2						
	U	PS	1.043 g/cm^3	0.85-1.00 mm	1.275 g	85%
	I	PVC	1.350 g/cm^3	0.85-1.00 mm	0.225 g	15%
Sample 3						
	U	PVC	1.350 g/cm^3	1.70-2.00 mm	2.125 g	85%
	I	PET	1.143 g/cm^3	1.70-2.00 mm	0.375 g	15%
Sample 4						
	U	PET	1.143 g/cm^3	1.70-2.00 mm	2.125 g	85%
	I	PVC	1.350 g/cm^3	1.70-2.00 mm	0.375 g	15%

materials, the desired product is expelled from the Multidune while the sterile product settles inside the chambers of the apparatus.

The choice of materials, their size and the operating flow rate was made based on the results of tests on mono-material samples (La Marca et al., 2011). Separation of PS and PVC particles ranging in size from 0.85-1 mm seems feasible using relatively low flow rates; under these conditions, PVC particles, which are heavier, are retained within the apparatus while PS ones tend to be expelled. For this reason, tests on Samples 1 and 2 were carried out with the water supply tank height set at Q1 or Q2, whereas tests on Samples 3 and 4, which involved PET and PVC plastic particles of larger size, were conducted using only the tank heights Q2 and Q3. For all samples, the duration of each experiment was approximately three minutes.

Fig. 9 shows the percentage in weight of material accumulated within each chamber and expelled through the output nozzles for all composite samples and hydraulic heads.

To quantify the separation efficacy, the following quantities are introduced:

-the grade of useful material in the useful fraction; this is equal to the ratio of the weight of the useful material to the total weight of the recovered useful fraction, expressed as a percentage; it provides an indication of the useful product and contaminant content in the concentrated product;

-the recovery of useful material; this is equal to the ratio of the weight of the recovered useful material to the weight of the useful material in the sample, expressed as a percentage; it permits the comparison of the amount of useful material in the concentrated product and in the sample;

-the concentration rate; this is equal to the ratio of the grade of the useful material in the concentrated product and the grade of the useful material in the sample; high values of the concentration rate, which varies between 1 and 1.176 (the grade of useful material in the sample is always equal to 85%), are associated with an efficient separation.

At the lowest flow rate (Q1), Sample 1 reaches a good level of purification. A high grade of PVC particles (99.18%) is achieved, and this is associated with a comparably high recovery value of 96.57%. The use of a higher flow rate is more problematic due to the excessive drag of heavier particles, determining a remarkable decrease of recovery of useful material from 96.57% to 66.12%.

Sample 2, primarily consisting of PS particles, is effectively purified using the lowest flow rate. A high grade (98.86%) is achieved and is associated with an excellent recovery of useful product (96.61%). At the higher flow rate (Q2), a consistent drag of PVC plastics toward the exit occurs (Fig. 9b); in this case, the recovery of the useful phase is almost complete (98.58%) but the material is too heavily contaminated by the PVC particles to be useful, decreasing grade (from 98.86% to 92.63%) and especially concentration rate (1.090). The recovery of the contaminant in the waste fraction (not shown in the table) was equal to 55.45%, in other words, at the higher flow rate Q2 almost half of the heavy particles are expelled from the device and contaminate the fraction of useful material. Clearly, the use of a flow rate larger than Q1 will determine a deterioration of the separation effectiveness of the apparatus. Remarkably, Q1 provides good results in view of the recovery of both materials.

The separation test of Sample 3 at Q2 leads to an optimal level of purification of the useful material (Fig. 9c), reaching a grade equal to 98.40% with an almost total recovery of material (99.10%). Separation at rate Q3 produces a small benefit in terms of grade, increasing it to 98.65%, but a decrease of the recovery, which is reduced to 93.72%. Remarkably, a higher hydraulic head could be justified in view of achieving a grade of close to 100% for the useful phase, although this decreases the recovery.

The separation test of Sample 4 at Q2 leads to an excellent level of purification of the useful material (grade equal to 99.56%) with recovery of up to 95.60% (Table 3), while higher hydraulic heads produce small advantages in terms of recovery of useful product (96.79%), with a small loss of grade (99.02%).

Table 3. Useful phase grade, useful phase recovery and concentration rate or enrichment for composite tests

Test	Useful phase grade (%)	Useful phase recovery (%)	Concentration rate
Sample 1-Q1	99.18	96.57	1.167
Sample 1-Q2	99.75	66.12	1.174
Sample 2-Q1	98.86	96.91	1.163
Sample 2-Q2	92.63	98.58	1.090
Sample 3-Q2	98.40	99.10	1.158
Sample 3-Q3	98.65	93.72	1.161
Sample 4-Q2	99.56	95.60	1.171
Sample 4-Q3	99.02	96.79	1.165

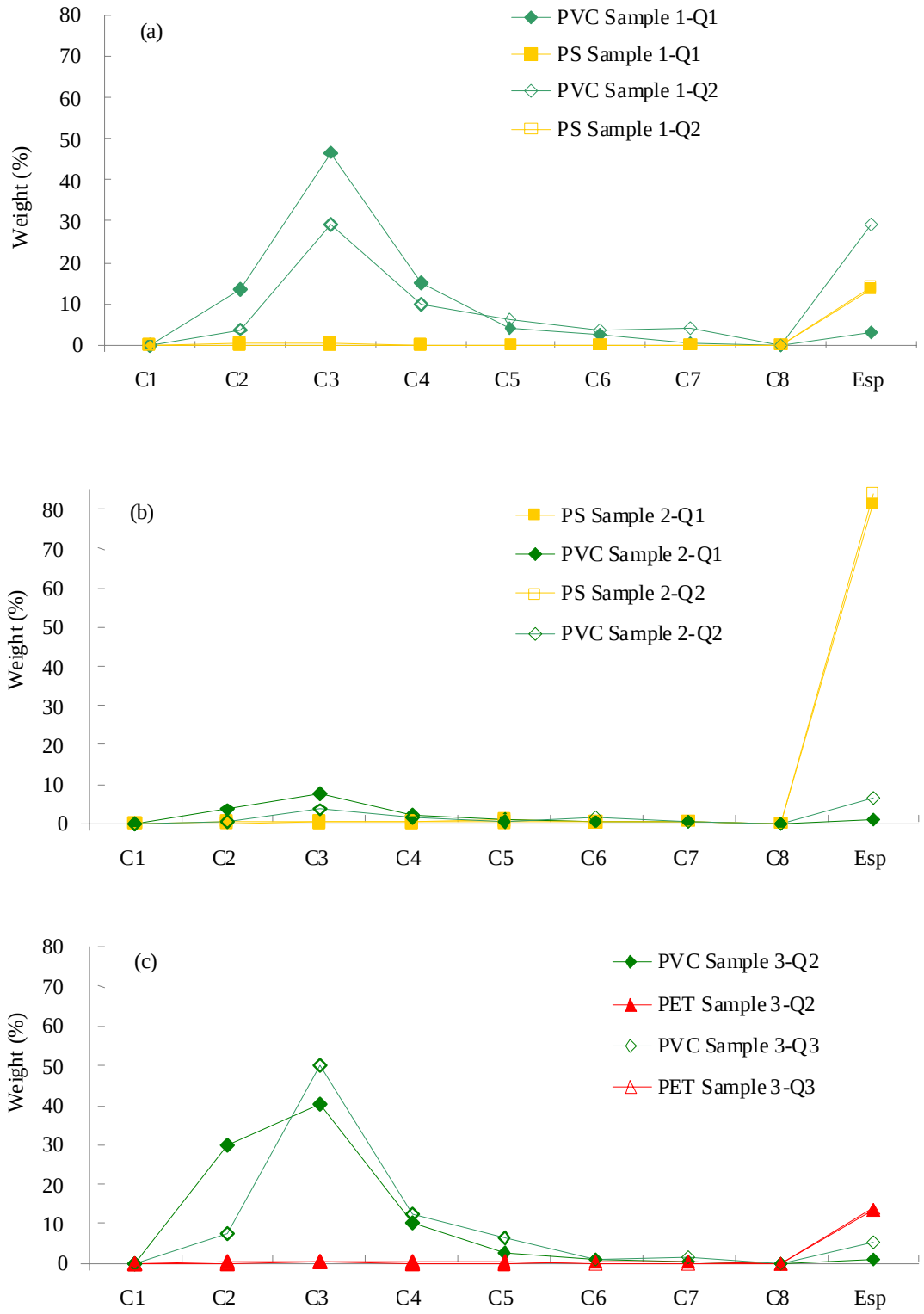

Fig. 9. Percentage in weight of materials accumulated in each chamber (R1-R8) and expelled through the output nozzles(Continues)

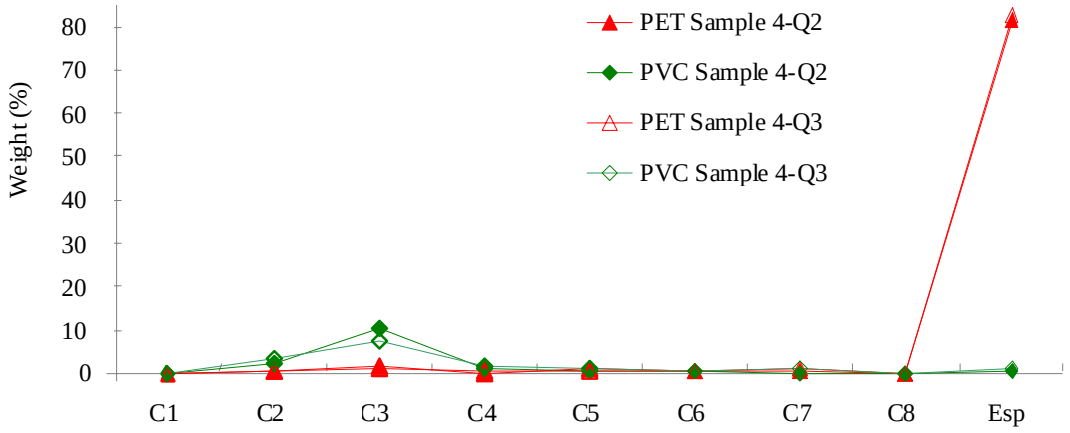

Fig. 9. Percentage in weight of materials accumulated in each chamber (R1-R8) and expelled through the output nozzles

Noticeably, Q2 optimizes the separation of the two materials in Sample 4, leading to extremely good results when both fractions must be recovered.

CONCLUSION

The high temporal and spatial resolution technologies employed for the reconstruction of the fluid-dynamic field inside the Multidune permits us to draw the following conclusions:

1.The flow field within the apparatus is characterized by three areas: the main transport current and recirculation areas above and below it in each chamber.

2.The fluid dynamic behavior is substantially similar in every chamber except the first and last ones (C1 and C8), in which the inlet and outlet nozzles prevent the formation of vortical structures.

3.The characteristic velocity of the principal current is significantly larger than the velocity within the upper and lower recirculation areas; this aspect is amplified with increasing hydraulic head at the apparatus inlet.

4.With variation in the hydraulic head, the geometry of the inner structures does not change appreciably; the size of vortices below and above remains basically unchanged.

5.An increase in the hydraulic head (and consequently in the flow rate) has a greater effect on the principal current rather than on the vortical structures within the chambers.

Tests on mono-material samples at different hydraulic heads allow an understanding of the influence of particle density and diameter on the behavior of sample particles inside the Multidune. Based on these tests, the following conclusions were made:

1.Light particles (PS and PET plastics) are expelled from the apparatus regardless of the hydraulic head; the influence of the particle size appears negligible.

2.The behavior of heavy particles (PVC) depends on both the hydraulic head and size. Smaller particles tend to settle only if the flow rate is low, while larger particles settle at each hydraulic head tested.

3.The largest amount of material always settles in the third chamber, regardless of the hydraulic head and type of material separated.

4.The amount of material settling in the first and last chambers is reduced due to the presence of inlet and outlet nozzles.

5.Particles that are not expelled tend to settle in the same chambers regardless of their density and diameter; this suggests that it is possible to achieve a differential separation of plastic particles only between expelled and settled material and not according to the chamber.

The analysis of images acquired using active tracer particles, i.e., the same plastic particles employed for both mono-material and composite sample separation tests, allowed us to observe the trajectories of particles within the Multidune. These results led to the following conclusions:

1.While traversing each chamber of the Multidune, particles interact with the lower recirculation area regardless of their density and average diameter; because lighter particles undergo an upward thrust and interact again with the principal current, they are therefore likely to proceed forward in the chambers and be expelled. Because heavier particles are more difficult to drag, they remain trapped in the chamber if the rotating motion is not particularly intense (i.e., at low flow rates). However, light and heavy particles always undergo rotating motion in the lower recirculation areas.

2.The velocity field is larger in C2 than elsewhere; separation is thus inhibited in C2, while particles tend to settle principally in C3.

3.Heavier particles tend to accumulate; if the hydraulic head is high enough, deposits are gradually eroded until the completion of material discharge.

4.The presence of settled material lessens the likelihood that new particles will settle, thus forcing particles to settle in the subsequent chambers.

Decontamination tests of composite samples confirmed the results of tests on mono-material samples. Plastic particles of different densities can be effectively separated if the flow rate is set to the appropriate value. Notably, reciprocal competition between particles of different specific mass is negligible, i.e., results obtained with composite samples are analogous to results obtained with mono-material samples.

REFERENCES

Adrian, R. J. (1991). Particle imaging techniques for experimental fluid mechanics. Annual Review of Fluid Mechanics, **23**, 261–304.

Ahmad, S. R. (2004). A new technology for automatic identification and sorting of plastics for recycling. Environmental Technology, **25 (10)**, 143–149.

Buchan, R. and Yarar, B. (1995). Recovering plastics for recycling by mineral processing techniques. The Journal of the Minerals, Metals & Materials Society, **47**, 52–55.

De Sena, G., Nardi, C., Cenedese, A., La Marca, F., Massacci, P. and Moroni, M. (2008). The Hydraulic Separator Multidune: Preliminary Tests On Fluid-Dynamic Features And Plastic Separation Feasibility. Waste Management, **28 (9)**, 1560-1571.

Dinger, P. (1992). Automatic sorting for mixed plastics. BioCycle, **33 (3)**, 80–2.

Gent, M. R., Menendez, M., Toraño, J. and Diego, I. (2009). Recycling of plastic waste by density separation: prospects for optimization. Waste Management and Research, **27**, 175-187.

Hearn, G. L. and Ballard, J. R. (2005). The use of electrostatic techniques for the identification and sorting of waste packaging materials. Resources, Conservation and Recycling, **44**, 91–98.

Horn, B. K. P. and Schunk, B. G. (1981). Determining optical flow. Artif. Intell., **17**, 185-203.

Jody, B. J. and Daniels, E. J. (2010). End-of-life Vehicle Recycling: The State of the Art of resource Recovery from Shredder Residue. ANL/ESD/07-8, 130 p. National Technical Information Service, US Department of Commerce, Springfield, VA 22161, USA. http://www.es.anl.gov/Energy_systems/publications/fact

Kinoshita, T., Okamoto, K., Yamaguchi, K. and Akita, S. (2006). Separation of plastic mixtures using liquid-fluidized bed technology. Chemosphere, **63**, 893–902.

La Porta, A., Voth, G. A., Crawford, A. M., Alexander, J. and Bodenschatz, E. (2001). Fluid particle accelerations in fully developed turbulence. Nature, **409**, 1017-1019.

Menéndez, M., Gent, M., Toraño, J. and Diego, I. (2007). Optimization of multigravity separation for recovery of ultrafine coal. Minerals & Metallurgical Processing, **24**, 253–263.

Moroni, M. and Cenedese, A. (2005). Comparison among feature tracking and more consolidated velocimetry image analysis techniques in a fully developed turbulent channel flow. Measurement Science and Technology, **16**, 2307-2322.

Moroni, M., Cushman, J. H. and Cenedese, A. (2003). A 3D-PTV Two-projection Study of Pre-asymptotic Dispersion in Porous Media which are Heterogeneous on the Bench Scale. International Journal of Engineering Science, **41 (3-5)**, 337-370.

Moroni, M., Kleinfelter, N. and Cushman, J. H. (2008). Alternative Measures of Dispersion Applied to Flow in a Convoluted Channel. Advances in Water Resources, **32 (5)**, 737-749.

Niblack, W. (1986). An introduction to digital image processing. (Prentice-Hall International).

Nogueira, J., Lecuona, A. and Rodríguez, P. A. (2001). Local ûeld correction PIV, implemented by means of simple algorithms, and multigrid versions. Measurement Science and Technology, **12**, 1911–1921.

Plastics International, (2007). Mechanical properties. Plastics International, Material properties, http://www.plasticsintl.com/sortable_materials.php?display=electrical (accessed 16 October 2008).

Plastics Europe, (2007a). An analysis of plastics production, demand and recovery for 2005 in Europe. PlasticsEurope, 21 pp.

Plastics Europe, (2007b). Press Release 9 May 2007, 1 p. Association of Plastics Manufacturers in Europe (AISBL), Brussels, Belgium.

Plastics Europe, (2010). Plastics - the Facts 2010, An analysis of European plastics production, demand and recovery for 2009. Association of Plastics Manufacturers in Europe (AISBL), Brussels, Belgium.

Raffel, M., Willert, C., Werely, S. and Kompenhans, J. (2007). Particle Image Velocimetry, A Practical Guide. (Heidelberg: Springer).

Sadat-Shojai, M. and Bakhshandeh, G. R. (2011). Recycling of PVC wastes. Polymer Degradation and Stability, **96**, 404-415.

Shent, H., Pugh, R. J. and Forssberg, E. (1999). A review of plastics waste recycling and the flotation of plastics. Resour. Conserv. Recy., **25**, 85–109.

Shindler, L., Moroni, M. and Cenedese, A. (2010). Spatial–temporal improvements of a two-frame particle-tracking algorithm. Measurement Science and Technology, **21**, 115401.

Tilmatine, A., Medles, K., Bendimerad, S. E., Boukholda, F. and Dascalescu, L. (2009). Electrostatic separators of particles: Application to plastic/metal, metal/metal and plastic/plastic mixtures. Waste Management, **29**, 228–232.

Wei, J. and Realff, M. J. (2005). Design and optimization of drum-type electrostatic separators for plastics recycling. Industrial and Engineering Chemistry Research, **44 (10)**, 3503–3509.

Welle, F. (2011). Twenty years of PET bottle to bottle recycling—An overview. Resources, Conservation and Recycling, **55 (11)**, 865-875.